



Assessment and management of interfraction variations of lumpectomy cavities in accelerated partial breast irradiation

Xiaojian Chen¹, Julia White¹, Wenhui Li², Ergun Ahunbay¹, Adam Currey¹, Carmen Bergom¹, Tracy Kelly¹, J. Frank Wilson¹, X. Allen Li¹

¹Department of Radiation Oncology, Medical College of Wisconsin, Wisconsin, USA; ²Department of Radiotherapy, Yunnan Tumor Hospital, Kunming 650221, China

Contributions: (I) Conception and design: XA Li, X Chen; (II) Administrative support: XA Li; (III) Provision of study material or patients: J White, C Bergom, T Kelly, JF Wilson; (IV) Collection and assembly of data: X Chen, W Li; (V) Data analysis and interpretation: X Chen, E Ahunbay, XA Li; (VI) Manuscript writing: All authors; (VII) Final approval of manuscript: All authors.

Correspondence to: X. Allen Li, PhD. Medical College of Wisconsin, Wisconsin, USA. Email: ALi@mcw.edu.

Background: The purpose of this study is to quantitatively characterize interfraction variations of lumpectomy cavity (LC) in accelerated partial breast irradiation (APBI) and their dosimetric impacts, and to explore the use of an online adaptive replanning scheme to address these variations.

Methods: A total of about 100 diagnostic-quality CT sets acquired using an in-room CT at each fraction during image-guided radiation therapy (IGRT) for ten randomly-selected patients treated with APBI in the supine position were analyzed. The LC, treated breast, lung and heart were delineated on each fraction CT. Organ volume change and deformation were quantified. For each fraction CT, three types of plans were created: adaptive, repositioning, and fully re-optimized plans. The plan qualities were compared.

Results: Significant changes in LC shape and volume were observed during APBI. On average, the LC volume decreases by 23% from the planning CT. The average change in LC shape, as measured by the Dice's coefficient, is 80%. For all patients, the adaptive plans were comparable to the re-optimization plans. For small and moderate LC changes (70%), the three types of plans were comparable, indicating that the current IGRT with the standard margins was sufficient to account for the interfraction variations. For cases with extreme LC change (30%), the adaptive plans offered improved target coverage and/or normal tissue sparing as compared with the repositioning plans.

Conclusions: Significant variations in the LC between planning and treatment were found for APBI. The current practice of IGRT with standard planning target volume margins can account for these variations for most cases. Online adaptive replanning was needed for cases with extremely large changes in LC.

Keywords: Adaptive RT; accelerated partial breast irradiation (APBI); interfraction anatomic variations; online replanning

Received: 01 December 2018; Accepted: 25 March 2019; Published: 04 April 2019.

doi: 10.21037/tro.2019.03.04

View this article at: <http://dx.doi.org/10.21037/tro.2019.03.04>

Introduction

A major challenge in the delivery of breast cancer radiotherapy (RT) for breast conserving therapy arises from the interfraction patient setup errors and anatomic variations including the changes from simulation to treatment delivery (1,2). Since the breast is composed of soft tissue that often has recently undergone surgical procedure(s), it is prone to

displacement and deformation between fractions (1,3). The size and shape of the lumpectomy cavity (LC) have been reported to vary substantially with time based upon the studies of LC contours as well as surgical clips (2-9). These variations result in either excessive dose to normal tissues or suboptimal dose coverage for the target, which can reduce the optimal coverage of targets and sparing organs at risk

that had been designed in the initial treatment plan (10,11). This dosimetric inaccuracy becomes even more critical for accelerated partial breast irradiation (APBI) as its total fractions are fewer and the prescribed dose per fraction is higher compared to whole breast irradiation.

To address the interfraction variations, many schemes have been proposed or developed. The most popular strategy is image-guided RT (IGRT), characterized by imaging and repositioning the patient prior to the delivery, based upon rigid-body registration. IGRT is introduced to reduce interfraction setup and translational variations in general (1,3,5). This conventional technique, however, is not capable of fully addressing organ deformation, target volume changes and the relative position shift between the target and critical organs. On the other hand, online replanning with a full-scale optimization based on the CT acquired for a specific fraction seems most appealing to achieve the ideal dose distribution for the fraction but this is currently not feasible practically, as it requires an unacceptable time length to generate a new plan. To address this issue, fast online adaptive RT (ART) strategies, where the original plan is modified based on the current fraction CT, were introduced (12-15). Such a fast replanning algorithm, for example, consists of segment aperture morphing (SAM) and segment weight optimization (SWO) (15-17). The SAM alters each intensity-modulated RT (IMRT) segment shape according to the change of the target from the planning CT to the CT of the day, while the SWO optimizes the weight of each new segment based on the pre-established dose-volume criteria. This scheme has been shown to effectively address interfraction changes in prostate cancer RT with acceptable replanning times (ranging from 8 to 12 minutes) (16). This strategy is also being explored for head and neck and pancreas cancers (15,17).

Although the interfraction changes in LC volume and shape for APBI have been previously studied, the dosimetric effects of these changes have only been sparsely reported. No effective correction strategy for such changes has been explored. The objectives of this work are (I) to characterize the interfraction variations for APBI in supine position based on CTs acquired at each fraction using an in-room CT (more accurate due to the diagnostic-quality CTs as compared to the cone-beam CTs used in most of the previous studies), (II) to thoroughly assess the dosimetric effects of these interfraction variations within the frame of IGRT technique, and (III) to evaluate the dosimetric effectiveness of using the SAM + SWO online ART strategy

to account for these variations.

Methods

This retrospective study was approved by the Institutional Review Board of the Medical College of Wisconsin. Analysis was completed on a total of about 100 diagnostic-quality CT sets acquired at each fraction using an in-room CT (CTVision, Siemens) during IGRT for ten patients treated with APBI in the supine position between 2008 to 2010. Among the 10 patients, 3 had a LC in the left breast and 7 in the right breast. Four of the patients had a LC located in the upper outer quadrant, 5 in the upper inner quadrant, and 1 in the lower outer quadrant. The patients were irradiated with a total dose of 38.5 Gy in 10 fractions in 5 days approximately 4–6 weeks after lumpectomy surgery. For each fraction CT set, the LC, treated breast, lungs and heart were delineated by populating the contours from the planning CT to the fraction CT using an auto-segmentation tool (ABAS, Elekta) based on deformable image registration (DIR) and then edited manually by two radiation oncologists. The clinical target volume (CTV) and the planning target volume (PTV) were created following the NSABP B-39/RTOG protocol 0413 with expansions of 1.5 and 2.5 cm from the LC, respectively. The PTV evaluation volume (PTV_EVAL) is defined by limiting the PTV to 5 mm from the skin and by the posterior breast tissue extent.

The interfraction variations, including the changes in organ volume and shape, were quantified with diverse parameters calculated with a software tool (Seg3D, Siemens). The definitions of these parameters are illustrated in *Figure 1*. The relative volume ratio (RVR), defined as the ratio of the volume in the fraction CT to that in the planning CT, is a direct measure of the relative volume change from the planning to each fraction. The shape changes in three dimensions (3D) [left-right (LR), anterior-posterior (AP), and superior-inferior (SI)] were analyzed with the bounding box method (18) for each fractional CT. In addition, the maximum overlap ratio (MOR), calculated between the volumes based on planning and fraction CTs for a given structure, and the Dice's coefficient (DC), the ratio of overlapping volume to the average volume of the planning and fraction contours, were used to evaluate shape and volume variations, i.e., excluding translational and rotational variations that can be accounted for by the IGRT repositioning. In this sense, MOR and DC were both used

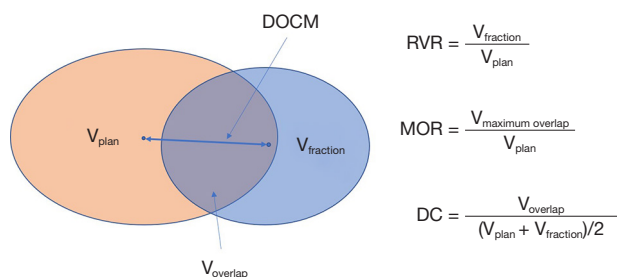


Figure 1 A schematic to illustrate the definitions of the relative volume ratio (RVR), the maximum overlap ratio (MOR), the Dice's coefficient (DC), and the distance of center of mass (DCOM). V_{plan} , V_{fraction} are the structure volumes in the planning CT and fraction CT. V_{overlap} is the overlap volume of these two. The maximum overlap volume ($V_{\text{maximum overlap}}$) is the volume under the condition that the positions of the two volumes are adjusted to give the maximum overlap.

to analyze deformations which cannot be fully corrected by IGRT. The distance of center of mass (DCOM) between LC and another organ, including treated breast and heart, was also used to measure relative geometry between these structures. A paired two-tailed t -test was used to obtain the significance of the changes from the planning CTs to the treatment CTs and interfraction variations. Pearson's r and Spearman rank correlation tests were used to test the linear and non-linear correlations.

For each fraction CT set, three types of plans were generated and compared to assess the dosimetric effect of the interfraction variations. The first type is the repositioning plan generated by applying the original plan with proper repositioning shifts to the fraction CT, which is usually registered to the planning CT based on the alignment of LCs and/or surgical clips (19). It has been shown that the clips represent a better surrogate for LC than the breast surface (3). As the diagnostic-quality CT allows visualizing both clips and LCs on most of the fraction CTs, two repositioning plans based on the two alignment methods were generated for each fraction CT. These repositioning plans represent the current standard IGRT practice. The second type of plan is the adaptive plan generated using an online replanning tool (RealART, Prowess) that uses the SAM and SWO algorithm described above (15-17). The third type of plan is the re-optimization plan obtained by a full-scale optimization based on the fraction CT using the same dose volume constraints used for the original plan. The re-optimization plan represents

the ideal solution. The plan quality for these three types of plans was compared based on dose-volume parameters.

The dose-volume constraints from NSABP B-39/RTOG 0413 protocol were adopted for the original IMRT, ART and re-optimization plans for each fraction. For the PTV_EVAL, the volume covered by 95% of the prescription dose (V_{95}) $\geq 95\%$ of the PTV_EVAL volume. For the ipsilateral breast reference volume, $V_{50} \leq 50\%$ and $V_{100} \leq 35\%$, for ipsilateral lung, $V_{30} < 15\%$, while $V_5 < 15\%$ for the contralateral lung and for heart, $V_5 < 5\%$ for right-side lesion and $V_{40} < 5\%$ for left-side lesion. For the contralateral breast and thyroid, the maximum point dose was limited to 3% of the prescribed dose.

To demonstrate cumulative dosimetric effects, an attempt was made to compute cumulative doses over all fractions for the four plans for a selected sample case. The deformable image registration matrices obtained between the CT of the first fraction and CTs of other fractions using the ABAS tool were used to map doses from fraction CTs to the CT of the first fraction. The cumulative dose was then obtained by summarizing the deformed fraction doses on the CT of the first fraction.

Results

As expected, the shape and volume of the LC changed substantially from the CT simulation to the treatment delivery. These changes persisted through all fractions with certain variations. A typical set of LC interfraction changes in a patient are shown in *Figure 2A*, where all fraction LC contours were overlaid onto the planning LC contour (red, thick line) in the axial view. *Figure 2B* shows the overlaid locations of the six surgical clips from the planning CT (blue, solid rings) and a fraction CT (yellow, dashed rings) for the same patient. Relative shifts from the positions of the clips in the planning CT to those in the fraction CT are different in both magnitude and direction, indicating LC deformation, in addition to the general volume shrinkage.

Details of the LC dimension changes can be determined by the bounding box method. For each fraction, the changes in the box dimensions along LR, AP, and SI directions were calculated. The histograms of those changes collected from all patients are displayed in *Figure 2C*. The average changes were -4.7 ± 3.4 , -3.1 ± 2.6 , and -2.5 ± 4.9 mm in LR, AP, and SI directions, respectively. These changes were random in nature. The overall histogram calculated based on LR, AP, and SI changes is also included in *Figure 2C*.

The RVRs and DCs for LCs calculated between the

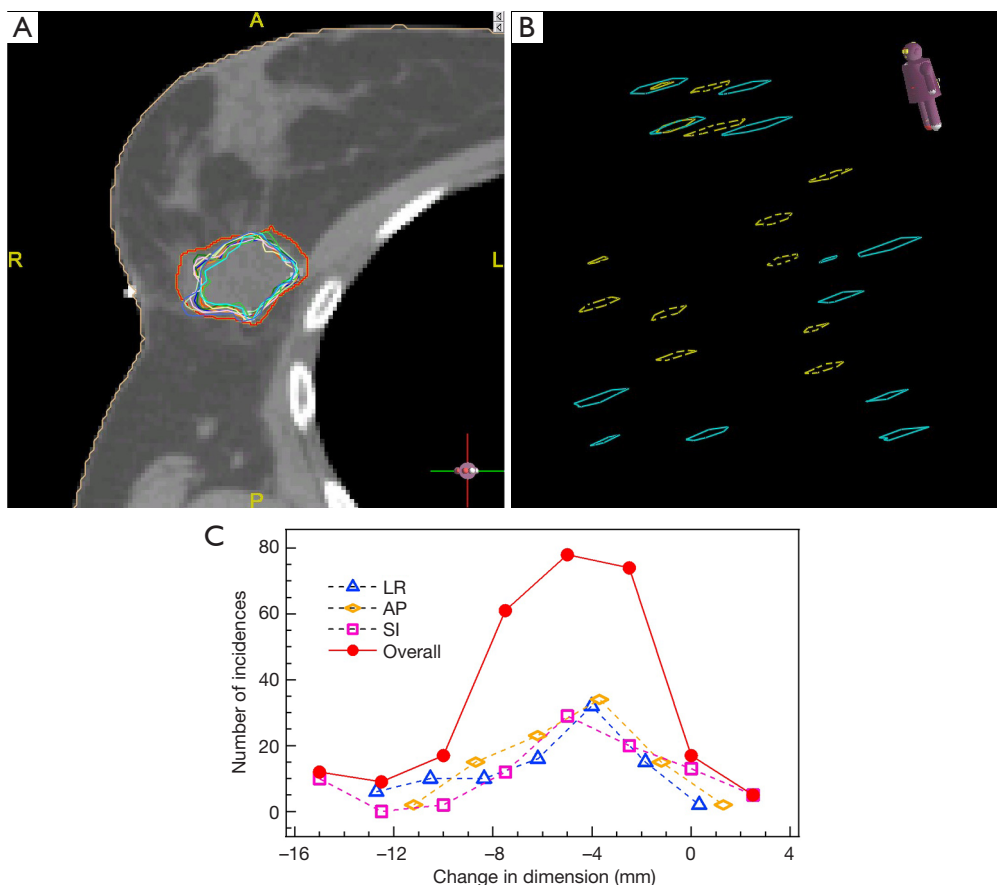


Figure 2 LC interfraction variations. (A) Axial view of the lumpectomy cavity contour from the planning CT (outermost, thick, red) overlaid with those from 10 fractional CTs (others) for a selected patient; (B) 3D view of two sets of clips. The rings represent the contours of the clips. One set was from the planning CT (blue, solid) and another set was from a fraction CT (yellow, dashed). Each set had 7 clips. They were aligned with the clip at the top-left corner. The slice spacing was 2.5 mm; (C) histograms of LC dimensional changes along the LR, AP, and SI axes with the red solid curve showing the overall distribution including all directions (sum of cases along LR, AP, and SI).

planning CTs and each of the 10 fractions for all 10 cases studied are shown in *Figure 3A* and *B*, respectively. Consistent with the trend illustrated in *Figure 2A*, the LC changed in the first fraction from the planning CT and remained relatively stable through the last fraction. The average values of RVR, MOR, and DC over 10 fractions for each of the 10 patients are shown in *Figure 3C*. On average, the volume of the LC at the last fraction is reduced by $23.0\% \pm 14.3\%$ [one standard deviation (SD)] from that in the planning CT for the 10 patients ($P=0.0004$). Compared to the changes from planning to the first fraction, the changes throughout the treatment course were small and fluctuated. The average of the SDs of the RVR values is $3.5\% \pm 1.9\%$, indicating the interfraction changes were negligible. The DC values range from 60% to 90% with

a mean value of $80.4\% \pm 6.0\%$. It was found that MOR and DC were both strongly correlated to RVR (both $P < 0.0001$, $r=0.99$ for MOR, and $r=0.94$ for DC based on Pearson's r correlation tests), suggesting their equivalence in measuring LC change. Although the LC changes observed in *Figure 3* unavoidably include the variation in the contour generation on fraction CTs, the contouring uncertainty should not be a major concern considering the total deviation of up to 50%.

The average values of RVR, MOR and DC for the treated breast volumes over the 10 patients are $98.8\% \pm 2.7\%$, $93.0\% \pm 2.0\%$ and $93.6\% \pm 1.0\%$, respectively, indicating relatively small shape and volume changes for the treated breasts from simulations to treatments. The average changes in DCOM between LCs and treated breasts and hearts are 2.3 ± 2.2 and 2.1 ± 1.3 mm, respectively.

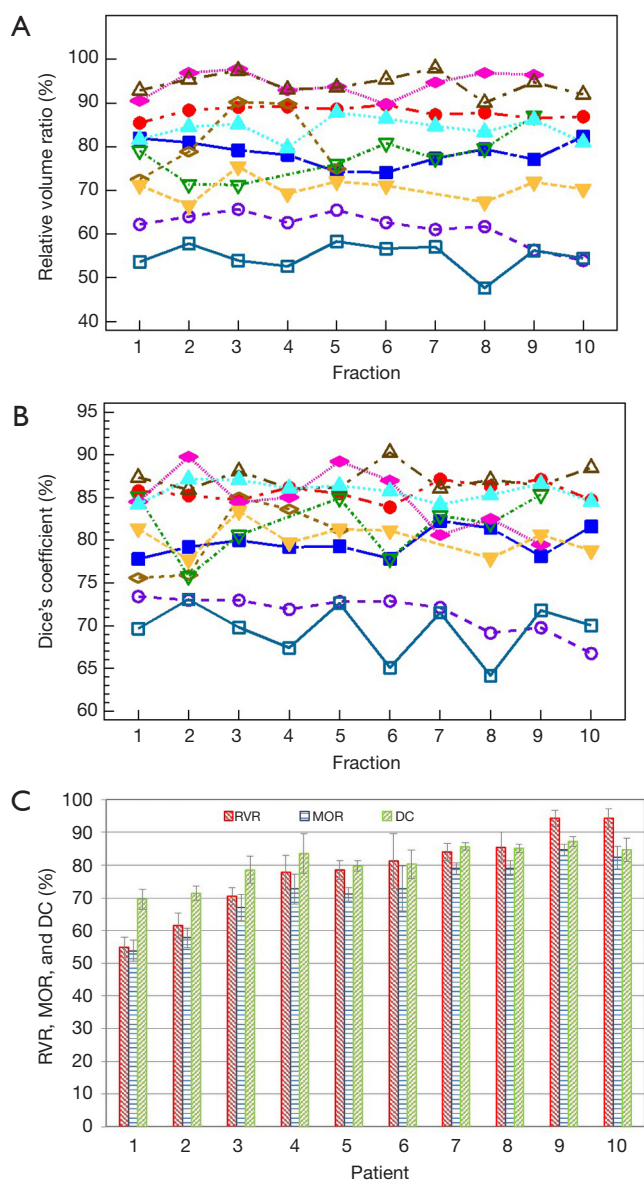


Figure 3 Interfraction changes of characteristic parameters. (A) Relative volume ratios (RVR) and (B) Dice's coefficients (DC) of lumpectomy cavities between the planning and fractional CT contours for 10 patients, and (C) the averages of RVRs, maximum overlap ratios (MOR) and DCs over all fractions for 10 patients. The error bars show the standard deviations obtained from 10 fractions.

In Figure 4, dose volume histograms (DVH) for the four plans (two repositioning plans based on surgical clip and LC alignments, adaptive plan, and re-optimization plan) generated for a fraction CT are compared for a case with relatively small LC changes (case #9 in Figure 3C). A relatively good agreement between the four plans indicates

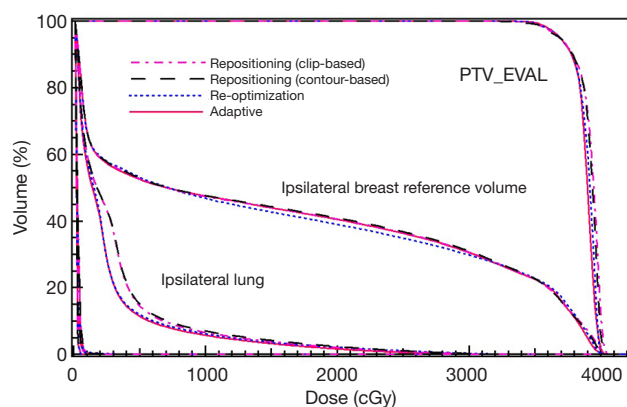


Figure 4 DVHs for two repositioning plans (the dash-dotted lines and the dashed lines for the clip-based and the LC-based plans, respectively), an adaptive plan (solid lines) and a re-optimization plan (dotted lines) generated based on one fraction CT for a case with small interfraction lumpectomy cavity changes.

that the dosimetric impact of the small LC changes is also small, and the repositioning method with IGRT is adequate to address the variation between simulations and deliveries. Since the LC volume variations did not change significantly between the initial and last fractions ($P=0.45$), the DVH behaviors for one fraction can approximately represent those for other treatment fractions.

The DVHs of the four plans generated for a case with relatively large LC changes (case #1 in Figure 3C) are shown in Figure 5. Clearly, the adaptive and re-optimization plans are similar, and both provide better plan qualities than the two repositioning plans. The DVHs for normal breast tissue and the treated breast excluding PTV_EVAL are shown in Figure 5B. The adaptive plan yields 11.0% and 5.2% reductions in the V_{50} of the normal breast tissue for the clip-based and LC-based plans, respectively. The same trend can also be seen for the heart as shown in Figure 5C, which is a zoom-in of the low dose region in Figure 5A.

Several key dose-volume parameters for the four plans generated based on one fraction CT for these cases with relatively large LC changes (cases #1–3 in Figure 3C, with LC volume shrinkage of $\geq 30\%$) and a case with small LC change (case #9 in Figure 3C, the case in Figure 4) are tabulated in Table 1. It is demonstrated again that the online ART plans are comparable to the re-optimization plans and both are better than the repositioning plans, in both target coverage and normal tissue sparing, for the cases with large LC changes.

Table 2 shows the average values of various dose-volume

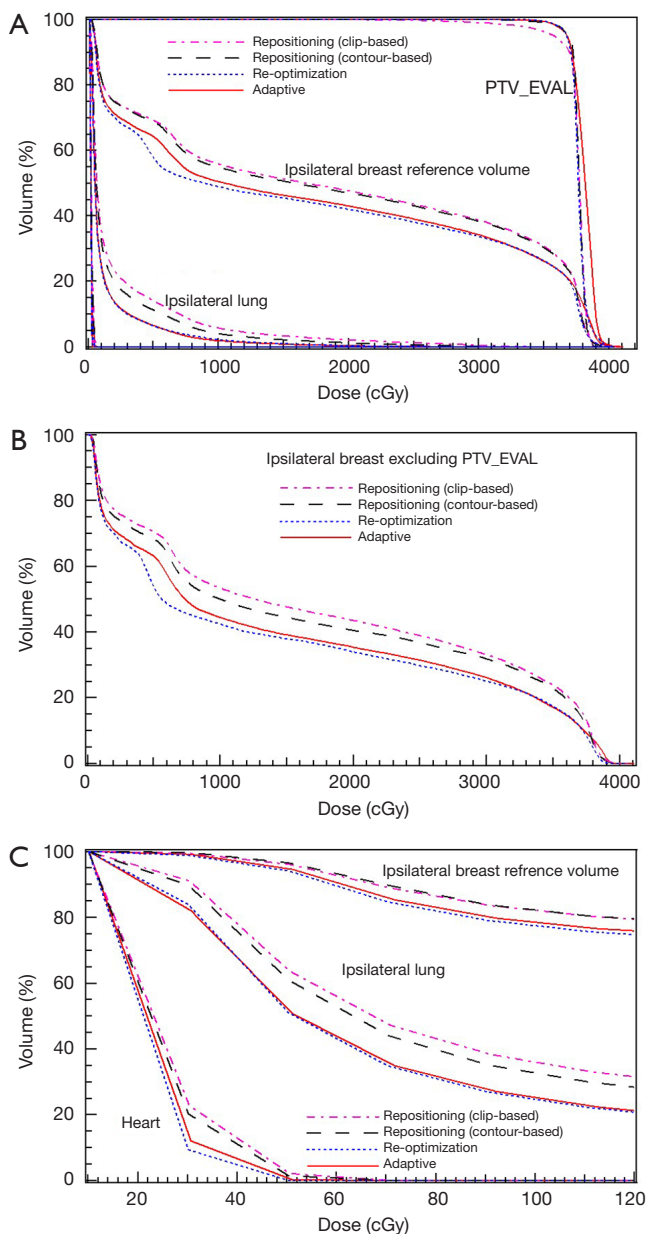


Figure 5 DVHs of the four plans generated based on one fraction CT for a case with relatively large lumpectomy cavity changes. (A) DVHs for all inspected structures. Details for normal breast tissue (treated breast excluding PTV_EVAL) and the heart are shown in (B) and (C), respectively.

parameters over all fractions for the four plans generated for each individual fraction for the 10 cases studied. Generally, the adaptive plans and the re-optimization plans are comparable and meet required dosimetric criteria (average P value of 0.32 ± 0.16 , ranging from 0.13

to 0.57, for all parameters), and both are better than the two repositioning plans. Specifically, the criterion of $V_{95} \geq 95\%$ for PTV_EVAL was met in only 50% of cases for the LC-based repositioning plans. Although not statistically significant, the repositioning plans based on LC contours are slightly better than those based on clips. For example, the average V_{95} for PTV_EVAL increases by 2.2%, and the average V_{50} for the healthy ipsilateral breast tissue decreases by 1.1% when comparing the LC-based to the clips-based repositioning plans. The smallest V_{95} values were observed for the three cases with large LC changes listed in *Table 1*. This can be understood that as the LC deformation becomes large, the changes in the clips' positions cannot accurately represent the changes in LC.

The cumulative doses calculated for a case with large LC changes (case #3) were obtained for the four plans. The obtained quantities based on the cumulative doses, in the order of the clip-based repositioning, LC-based repositioning, adaptive, and re-optimization plans, were 80.9%, 90.9%, 95.5%, and 95.4% for the PTV_EVAL V_{95} ; 35.7%, 31.9%, 30.3%, and 28.9% for the V_{50} normal breast tissue (excluding PTV_EVAL) and 11.8%, 9.3%, 6.7%, and 8.5% for the ipsilateral lung V_{30} , respectively. These values are basically consistent with those obtained for the first fraction, indicating that the above observations based on fraction doses are generally applicable for those based on cumulative doses.

Discussion

Change in LC shape and size during post-operative radiation therapy for breast cancer is well-known and has been extensively studied (4,6,20-22). The LC volume is generally decreased from simulation to treatment. In this study, the change in LC volume from the planning CT to the fraction CTs varies from 5–50%, similar to those reported by others (4). This change can lead to dosimetric deviation from the prescribed plan. To address this issue, adaptive planning has been reported for the LC boost treatment following whole breast irradiation (WBI) (2,8,23,24). In this study, the benefits of adaptive planning for APBI, which uses the LC as a CTV, have been explored with similar trends and conclusions obtained regarding to maintaining the PTV coverage and reducing the dose of OARs.

For the cohort in this study receiving APBI, the benefit of ART is evident for 30% of the patients who have a large LC shrinkage, comparable to 26% observed for WBI (24).

Table 1 Dose-volume quantities of four plans generated for one case (case 9) with small LC change and three cases (cases 1, 2 and 3) with large LC changes based on one fraction CT. The V_5 of the hearts and the contralateral lungs had a zero value for all 4 cases (not shown)

Case No.	Structure	Quantity	Repositioning		Adaptive	Re-optimization
			Clip	LC contour		
9	PTV_EVAL	V_{95}	95.5	95.5	95.9	95.9
	Breast reference volume (ipsi)	V_{50}	41.0	41.4	41.0	39.6
	Breast (ipsi) – PTV_EVAL	V_{100}	5.2	4.3	3.6	3.1
	Breast (ipsi) – PTV_EVAL	V_{50}	46.6	46.2	46.3	45.6
	Lung (ipsi)	V_{30}	5.5	5.9	4.8	5
1	PTV_EVAL	V_{95}	91.8	96.2	95.9	95.9
	Breast reference volume (ipsi)	V_{50}	48.1	47.4	43.5	42.5
	Breast (ipsi) – PTV_EVAL	V_{100}	2.1	1.9	4.4	1.0
	Breast (ipsi) – PTV_EVAL	V_{50}	44.0	40.9	35.9	34.6
	Lung (ipsi)	V_{30}	4.6	3.2	1.4	1.4
2	PTV_EVAL	V_{95}	86.1	88.5	95.4	95.5
	Breast reference volume (ipsi)	V_{50}	46.1	46.1	42.5	45.2
	Breast (ipsi) – PTV_EVAL	V_{100}	10.5	5.6	8.8	3.6
	Breast (ipsi) – PTV_EVAL	V_{50}	56.5	50.7	45.5	48.6
	Lung (ipsi)	V_{30}	2.4	2.3	2.2	2.6
3	PTV_EVAL	V_{95}	86.7	93.0	95.6	95.9
	Breast reference volume (ipsi)	V_{50}	42.4	41.4	37.9	40.1
	Breast (ipsi) – PTV_EVAL	V_{100}	0.6	0.2	0.3	0.1
	Breast (ipsi) – PTV_EVAL	V_{50}	36.1	32.1	28.5	29.7
	Lung (ipsi)	V_{30}	12.2	9.4	7.6	7.9

Breast (ipsi) – PTV_EVAL, ipsilateral breast excluding PTV_EVAL.

Table 2 Average values of dose-volume quantities over all fractions for four plans generated for each individual fraction for the 10 cases studied

Structure	Quantity	Requirement	Repositioning		Adaptive	Re-optimization
			Clip	LC contours		
PTV_EVAL	V_{95}	$\geq 95\%$	92.3 \pm 3.6	94.5 \pm 2.5	95.7 \pm 0.1	95.8 \pm 0.1
Breast reference volume (ipsi)	V_{50}	$\leq 50\%$	43.0 \pm 5.2	43.1 \pm 5.0	41.6 \pm 5.3	41.6 \pm 5.4
Breast (ipsi) – PTV_EVAL	V_{100}	N/A	3.3 \pm 3.0	3.2 \pm 2.2	3.6 \pm 2.8	2.5 \pm 1.9
Breast (ipsi) – PTV_EVAL	V_{50}	N/A	43.2 \pm 10.2	42.1 \pm 10.0	40.6 \pm 9.6	40.0 \pm 9.7
Breast reference volume (contra)	Maximum	As low as possible	7.8 \pm 5.3	7.2 \pm 5.7	6.3 \pm 5.5	7.2 \pm 6.8
Lung (ipsi)	V_{30}	$\leq 15\%$	5.3 \pm 3.6	5.0 \pm 2.8	3.9 \pm 2.4	4.2 \pm 2.8
Lung (contra)	V_5	$\leq 15\%$	0.0 \pm 0.0	0.0 \pm 0.0	0.1 \pm 0.3	0.0 \pm 0.0
Heart	V_5	$\leq 5\%$	0.6 \pm 1.1	0.3 \pm 0.8	0.3 \pm 0.9	0.2 \pm 0.7

For the remaining 70% of patients without large LC changes, the two repositioning plans were generally concordant with minor differences between them (P values were 0.056 for target coverage, 0.040 for normal breast tissue sparing, and 0.17 for lung tissue sparing). The reason ART is not necessary for all patients partially lies in the fact that the relatively small or moderate LC deformations or volume changes are accounted for in the margins used to define PTV and PTV_EVAL. The PTVs generated with a large expansion (25 mm) from the LC and the PTV_EVAL trimmed from the PTV were much larger than LCs, with the average volume ratios of PTV/LC and PTV_EVAL/LC of 18.3 ± 6.1 and 11.1 ± 3.6 , respectively. In addition, the trimming for PTV_EVAL along the curvature of the breast cause a further loss of the inherent geometric characteristics of LC. It is reasonable to argue whether such large CTV to PTV margins are necessary for the ART plan as it can account for target volume and shape changes. With a reduced PTV margin, the benefit of ART would be increased, even for the case with moderate changes in LC. For the studied cohort, the threshold of RVR for ART is roughly 70%. This value is close to the one obtained in the study of adaptive planning for the boost after whole breast irradiation, which is 65% (24). For the patients who have an RVR smaller than 70% at the first treatment, ART would be recommended. If RVR is greater than 70%, IGRT should be sufficient.

It should be noted that the change of the breast volume is generally not a concern as it is not significantly changed (20,25). In this study the treated breast volumes had a median volume of 842.9 cm^3 and an interquartile range from 635.5 to 928.7 cm^3 , which is in normal range for early-stage breast cancer patients (26) as a result of random selection of patients. The RVR of breast volumes over the 10 patients averaged 98.8%, which indicates a very minor change.

The timeline of the treatment flow is critical for the option of adaptive planning. In this study, the CT simulations were performed 2–8 weeks after surgery and usually 2 weeks before treatment of the first fraction. The decrease in LC volume depends strongly on the surgery-to-simulation time span (spearman rank correlation test, $r = -0.89$, $P = 0.003$), which is consistent with the previous reports (20,21). The change, however, does not depend on the simulation-to-treatment time span ($r = 0.24$, $P = 0.57$). It is known the LC volume increases first, due to seroma filling, and then decreases as seroma is reabsorbed after lumpectomy (4). The LC volume usually reaches its peak

2–4 weeks after the lumpectomy and then decreases with a continuously reduction rate with time. The change stabilizes at 9–14 weeks after surgery (27). If the simulation was performed at a time with peak LC volume, a severe LC change would be expected. For the cases studied with a surgery-to-simulation time span less than 3 weeks, reductions in LC volume were greater than 25% suggesting that CT simulation should be performed at least 3 weeks after lumpectomy to avoid extreme LC changes. If simulation is performed within 3 weeks of the lumpectomy, online ART may be considered as the LC is likely to experience a larger interfraction change. Unlike WBI, the treatment course of APBI only takes 5 days, and therefore the change of LC during the course is minimal as reflected in *Figure 2A* and *B*. The difference between the first and last fraction is not significant for RVR ($P = 0.45$) and DC ($P = 0.75$). The online ART can be performed on the first fraction and the adaptive plan can be extendedly used for the remaining fractions.

One major limitation of this study is the small cohort size. Also, this study presents an explorative view of the merits of ART. It may not cover all types of cases in actual clinical practice. For example, the location of the LC, and the distance between the LC and heart in extreme cases could lead to a difference in the dosimetric effects seen. The distribution of the existing cases in the cohort may deviate from reality and therefore the statistics of the ART benefits based on the patients may not be representative for all patients. For example, in contrast to the fact that slightly more breast tumors are in the left breast than the right (28), only 3 of out of 10 patients has a LC on the left breast, where the heart dose is a more concern than the right breast patients. Compared to literature (29), the number of cases with a LC in the upper inner quadrant was relatively over-weighted which increased the difficulty of sparing the contralateral breast.

Conclusions

The interfraction anatomic variations in patients with APBI in the supine position were qualitatively analyzed. Significant volume shrinkage and deformations in LC were observed, particularly at the first fraction. While the current practice of IGRT repositioning can account for the variations for a large proportion of the cases studied owing to the large PTV margin, the online ART was found to be advantageous for cases with extremely large LC changes. The IGRT plans based upon LC alignment are slightly

better than those based upon surgical-clip alignment. Online adaptive replanning is suggested at least for the first fraction for the cases with large LC changes.

Acknowledgments

Funding: This work is supported partially by the Susan G. Komen® Foundation. Inputs from Drs. Natalya Morrow, Jiyong Qin, Ya Li, Xiang Ding, and Yunhe Ju are greatly appreciated.

Footnote

Conflicts of Interest: All authors have completed the ICMJE uniform disclosure form (available at <http://dx.doi.org/10.21037/tro.2019.03.04>). Dr. White reports grants from Susan Komen Breast Cancer Foundation, during the conduct of the study. Dr. Li reports grants from Susan Komen Breast Cancer Foundation, during the conduct of the study; grants from Elekta Inc, grants from Siemens, outside the submitted work. The other authors have no conflicts of interest to declare.

Ethical Statement: The authors are accountable for all aspects of the work in ensuring that questions related to the accuracy or integrity of any part of the work are appropriately investigated and resolved. The study was conducted in accordance with the Declaration of Helsinki (as revised in 2013). This retrospective study was approved by the Institutional Review Board of the Medical College of Wisconsin. Informed consent was waived due to the retrospective nature of the study.

Open Access Statement: This is an Open Access article distributed in accordance with the Creative Commons Attribution-NonCommercial-NoDerivs 4.0 International License (CC BY-NC-ND 4.0), which permits the non-commercial replication and distribution of the article with the strict proviso that no changes or edits are made and the original work is properly cited (including links to both the formal publication through the relevant DOI and the license). See: <https://creativecommons.org/licenses/by-nc-nd/4.0/>.

References

- Morrow NV, Stepaniak C, White J, et al. Intra- and Interfractional Variations for Prone Breast Irradiation: An Indication for Image-Guided Radiotherapy. *Int J Radiat Oncol Biol Phys* 2007;69:910-7.
- Alderliesten T, den Hollander S, Yang TJ, et al. Dosimetric impact of post-operative seroma reduction during radiotherapy after breast-conserving surgery. *Radiother Oncol* 2011;100:265-70.
- Hasan Y, Kim L, Martinez A, et al. Image Guidance in External Beam Accelerated Partial Breast Irradiation: Comparison of Surrogates for the Lumpectomy Cavity. *Int J Radiat Oncol Biol Phys* 2008;70:619-25.
- Kim LH, Vicini F, Yan D. What Do Recent Studies on Lumpectomy Cavity Volume Change Imply for Breast Clinical Target Volumes? *Int J Radiat Oncol Biol Phys* 2008;72:1-3.
- Topolnjak R, de Ruiter P, Remeijer P, et al. Image-Guided Radiotherapy for Breast Cancer Patients: Surgical Clips as Surrogate for Breast Excision Cavity. *Int J Radiat Oncol Biol Phys* 2011;81:e187-e195.
- Jacobson G, Betts V, Smith B. Change in volume of lumpectomy cavity during external-beam irradiation of the intact breast. *Int J Radiat Oncol Biol Phys* 2006;65:1161-4.
- Penninkhof J, Quint S, Boer Hd, et al. Surgical clips for position verification and correction of non-rigid breast tissue in simultaneously integrated boost (SIB) treatments. *Radiother Oncol* 2009;90:110-5.
- Mohiuddin MM, Nichols EM, Marter KJ, et al. Decrease of the lumpectomy cavity volume after whole-breast irradiation affects small field boost planning. *Med Dosim* 2012;37:339-43.
- Ahunbay EE, Robbins J, Christian R, et al. Interfractional Target Variations for Partial Breast Irradiation. *Int J Radiat Oncol Biol Phys* 2012;82:1594-604.
- Hasan Y, Kim L, Wloch J, et al. Comparison of Planned Versus Actual Dose Delivered for External Beam Accelerated Partial Breast Irradiation Using Cone-Beam CT and Deformable Registration. *Int J Radiat Oncol Biol Phys* 2011;80:1473-6.
- Baroni G, Garibaldi C, Scabini M, et al. Dosimetric effects within target and organs at risk of interfractional patient mispositioning in left breast cancer radiotherapy. *Int J Radiat Oncol Biol Phys* 2004;59:861-71.
- Mohan R, Zhang X, Wang H, et al. Use of deformed intensity distributions for on-line modification of image-guided IMRT to account for interfractional anatomic changes. *Int J Radiat Oncol Biol Phys* 2005;61:1258-66.
- Fu W, Yang Y, Yue NJ, et al. A cone beam CT-guided online plan modification technique to correct interfractional anatomic changes for prostate cancer IMRT

- treatment. *Phys Med Biol* 2009;54:1691.
14. Li XA, Liu F, Tai A, et al. Development of an online adaptive solution to account for inter- and intra-fractional variations. *Radiother Oncol* 2011;100:370-4.
 15. Wu C, Jeraj R, Lu W, et al. Fast treatment plan modification with an over-relaxed Cimmino algorithm. *Med Phys* 2004;31:191-200.
 16. Ahunbay EE, Peng C, Holmes S, et al. Online Adaptive Replanning Method for Prostate Radiotherapy. *Int J Radiat Oncol Biol Phys* 2010;77:1561-72.
 17. Liu F, Erickson B, Peng C, et al. Characterization and Management of Interfractional Anatomic Changes for Pancreatic Cancer Radiotherapy. *Int J Radiat Oncol Biol Phys* 2012;83:e423-e429.
 18. Glide-Hurst CK, Gopan E, Hugo GD. Anatomic and Pathologic Variability During Radiotherapy for a Hybrid Active Breath-Hold Gating Technique. *Int J Radiat Oncol Biol Phys* 2010;77:910-7.
 19. Kim LH, Wong J, Yan D. On-Line Localization of the Lumpectomy Cavity Using Surgical Clips. *Int J Radiat Oncol Biol Phys* 2007;69:1305-9.
 20. Cho H, Kim C. Volumetric changes in the lumpectomy cavity during whole breast irradiation after breast conserving surgery. *Radiat Oncol J* 2011;29:277-82.
 21. Jeon SH, Shin KH, Park SY, et al. Seroma change during magnetic resonance imaging-guided partial breast irradiation and its clinical implications. *Radiat Oncol* 2017;12:103.
 22. Sharma R, Spierer M, Mutyala S, et al. Change in Seroma Volume During Whole-Breast Radiation Therapy. *Int J Radiat Oncol Biol Phys* 2009;75:89-93.
 23. Hurkmans CW, Dijkmans I, Reijnen M, et al. Adaptive radiation therapy for breast IMRT-simultaneously integrated boost: Three-year clinical experience. *Radiother Oncol* 2012;103:183-7.
 24. Chen X, Qiao Q, DeVries A, et al. Adaptive Replanning to Account for Lumpectomy Cavity Change in Sequential Boost After Whole-Breast Irradiation. *Int J Radiat Oncol Biol Phys* 2014;90:1208-15.
 25. Prendergast B, Indelicato DJ, Grobmyer SR, et al. The Dynamic Tumor Bed: Volumetric Changes in the Lumpectomy Cavity During Breast-Conserving Therapy. *Int J Radiat Oncol Biol Phys* 2009;74:695-701.
 26. Hoe AL, Mullee MA, Royle GT, et al. Breast size and prognosis in early breast cancer. *Ann R Coll Surg Engl* 1993;75:18-22.
 27. Kader HA, Truong PT, Pai R, et al. When Is CT-Based Postoperative Seroma Most Useful to Plan Partial Breast Radiotherapy? Evaluation of Clinical Factors Affecting Seroma Volume and Clarity. *Int J Radiat Oncol Biol Phys* 2008;72:1064-9.
 28. Perkins CI, Hotes J, Kohler BA, et al. Association between Breast Cancer Laterality and Tumor Location, United States, 1994–1998. *Cancer Causes Control* 2004;15:637-45.
 29. Rummel S, Hueman MT, Costantino N, et al. Tumour location within the breast: Does tumour site have prognostic ability? *Ecancermedalscience* 2015;9:552.

doi: 10.21037/tro.2019.03.04

Cite this article as: Chen X, White J, Li W, Ahunbay E, Currey A, Bergom C, Kelly T, Wilson JF, Li XA. Assessment and management of interfraction variations of lumpectomy cavities in accelerated partial breast irradiation. *Ther Radiol Oncol* 2019;3:13.